Retention Behaviors of Block Copolymers in Liquid Chromatography at the Critical Condition

Wenhua Jiang, Shazia Khan, and Yongmei Wang*

Department of Chemistry, The University of Memphis, Memphis, Tennessee 38152-3550

Received April 27, 2005; Revised Manuscript Received June 9, 2005

ABSTRACT: The partitioning of a diblock copolymer (AB) and a triblock copolymer (ABA and BAB) into a pore, at a condition similar to that employed in the experimental liquid chromatography at the critical condition (LCCC), was investigated by lattice Monte Carlo simulations with self-avoiding-walk chains. The B block is set at the predetermined critical condition where the partition coefficient of a homopolymer B has a least dependence on its chain length, and hence becomes chromatographically "invisible". The A block is set at the size-exclusion mode and is chromatographically "visible". The partition coefficients of these copolymers were compared with that of a homopolymer A with the same (total) length of the visible A block(s). The partition coefficient of a diblock, K_{AB}, was found to be larger than K_A, especially when the A block was short and the B block was long. The difference tends to vanish with an increase in the A block length or a decrease in the B block length. A smaller pore also tends to decrease the difference between the two. For the triblock copolymers, the partition coefficient for BAB, K_{BAB}, was found to be larger than K_A and was almost equal to K_{AB}, but the partition coefficient of ABA, K_{ABA}, was found be smaller than K_A. These simulation results are in remarkable agreement with experimental observations. As a result, the length of the visible block in diblock copolymer AB and triblock copolymer BAB would be underestimated, and that in triblock copolymer ABA would be overestimated in LCCC. The origins of these observed differences in partition coefficients are explained.

Introduction

Block copolymers are composed of sequences ("blocks") of the same monomer unit covalently linked to sequences of an unlike type at its end,[1,2] such as in diblock copolymers AB, triblock copolymers (ABA or BAB), and multiblock copolymers $(AB)_n$, where A and B represent different types of blocks. These block copolymers possess unique properties originating from their special architectures and have found important uses. For example, block copolymers form micelles and are used in drug delivery.[3,4] Asymmetric diblock copolymers serve as good templates for nanowire arrays.[5] Block copolymers are also frequently used to modify interfacial properties.[6,7]

The properties of block copolymers depend on the chemical structures of the repeat units as well as the architectural arrangements of the repeat units.[6−8] The microphase morphology formed by diblock copolymers depends critically on the relative length of the two incompatible blocks.[8] Hence, it is important to know not only the overall molecular weight of the block copolymers, but also either the molecular weight of each individual block or the chemical composition of the block copolymers. Size-exclusion chromatography (SEC) cannot provide information on the chemical composition since the hydrodynamic volume of a diblock copolymer chain is affected by both the molecular weight and the chemical composition.[9] Liquid chromatography at the critical condition (LCCC) has been proposed as a promising method to characterize individual blocks in block copolymers.[9] The idea of LCCC is to find a special condition, termed the "critical condition", where the elution of the homopolymer in the column could become independent of its molecular weight. When one of the blocks is set at such a critical condition, that block may be deemed as chromatographically invisible; thereby the retention of the block copolymer chain may be solely dependent on the visible block(s). The standard calibration method can then be used to determine the molecular weight distribution of the visible blocks. Zimina and his colleagues[10] took block copolymers of poly(styrene-*b*-methyl methacrylate) and poly(styrene-*b*-*tert*-butyl methacrylate) as examples and successfully performed the characterization of these block copolymers through LCCC. Others have also reported the usefulness of LCCC in estimating the molecular weights of the individual blocks in block copolymers,[11] as well as in separating polymers according to functionalities and other structural features.[12,13]

The theoretical predictions of chromatographic invisibility were given by Gorbunov and Skvortsov[14,15] for a Gaussian chain in continuum space and by Guttman et al.[16] for a random walk chain on the lattice. In both theoretical approaches, the monomer overlaps between segments are allowed, a simplification that has to be made in these theoretical studies. According to the theories, the critical condition in the liquid chromatography of polymers represents the thermodynamic state where the entropic size-exclusion effect of the polymer is precisely compensated by the enthalpic interaction of the polymer with the pore surface, which renders the partition coefficient of polymer between the confined solution in the pore and the bulk solution to become unity and completely independent of the molecular weight of the polymer. When one of the blocks (for example, the B block) of the block copolymer is rendered invisible, theories predict that the partition coefficient of the AB diblock copolymer K_{AB} and of BAB triblock K_{BAB} are the same as that of the homopolymer A with the same length. Accordingly, if the elution of polymers in LCCC is governed entirely by the distribution coefficient K (a condition called "quasi-equilibrium", which

* Corresponding author. Telephone: (901) 678-2629. Fax: (901) 678-3447. E-mail: ywang@memphis.edu.

10.1021/ma050899a CCC: $30.25
Published on Web 07/21/2005

is believed to be held in these chromatographic separations), then the estimations of the molecular weight of the A block in AB diblock copolymer and BAB triblock copolymers should be accurate in LCCC. For the ABA type, however, Guttman et al.[16] and recently Gorbunov and Vakhrushev[17] found that K_{ABA} is less than K_{AB}, K_{BAB}, or K_A. Accordingly, theory predicts ABA would elute earlier than BAB, AB, or A.

While many experimental results are in agreement with the theoretical predictions,[10,11] a few studies are not in complete agreement. Chang and co-workers have prepared a series of polystyrene-*b*-polyisoprene diblock copolymers with well-controlled molecular weight distributions of the blocks (determined through NMR) and compared the elution time of the block copolymers with that of the homopolymer precursor when the other block is set at the critical condition.[18] The elution times of the diblock were found to be longer than that of its homopolymer precursor and the elution time increased with an increase of the invisible block length. As a result, LCCC had underestimated the molecular weight of the visible blocks, and these underestimations were more significant when the visible blocks were relatively shorter than the invisible blocks. In another study, they prepared a set of polystyrene (PS)/polybutadiene (PB) block copolymers with similar molecular weight distributions and chemical composition distributions, but in different architectures: PS-*b*-PB (SB), PS-*b*-PB-*b*-PS (SBS), and PB-*b*-PS-*b*-PB (BSB).[19] When the PB block is set at the critical condition, they found SBS eluted significantly earlier than SB and BSB, which is in partial agreement with the theoretical predictions. The observed effects of the invisible blocks on the elution behavior of the visible blocks in these studies, especially in the cases of AB and BAB types of copolymers, were not very well understood and were sometimes debated.[17]

Several studies[20,21] have used computer simulations to investigate the critical condition employed in LCCC, including our own earlier reports.[22,23] In the absence of excluded volume interaction, the simulation yields the same result as that predicted by the previous theories, namely at the critical adsorption point, which is identified as the critical point, $K = 1$, and is independent of the chain length of the polymer. However, the inclusion of excluded volume interaction gives rise to some subtle yet important differences. First, the definition of the critical condition needs to be revised. We define the critical condition as the point at which the partition coefficient of the homopolymer is least dependent on its chain length. This is necessary because for the self-avoiding walk chains there is no point at which the partition coefficient is completely independent of the chain length. This definition of the critical condition is similar to that employed in experiments. Following this definition, we found that the critical condition in a slit pore is at the critical adsorption point ($\epsilon_w = -0.276$; ϵ_w is the reduced monomer/wall interaction) and it does not shift with the pore size.[22,23] The critical condition in a square channel pore, however, shifts with the pore size. In both types of pore, $K > 1$ at the critical condition. Our definition of the critical condition is in contrast to a more commonly used theoretical definition of the critical condition, the point at which $K = 1$. It is of interest to examine if the discrepancy between experimental results and the theoretical predictions could be attributed to the same excluded volume interaction ignored in the theory and to assess the extent to which the corrections from the excluded volume interactions should be included.

Simulation Method

All Monte Carlo simulations were conducted in a simple cubic lattice. Polymer chains were modeled as self-avoiding walks on the lattice. The partition coefficients, K, were determined from the chemical potential difference of a polymer chain in a confined solution and in a bulk solution, $-\ln K = \beta(\mu_{conf} - \mu_{bulk})$, where μ_{conf} and μ_{bulk} represent the excess chemical potential of the chain in the confined solution and in the bulk solution with respect to the same reference state, respectively.[22,23] This method is only valid in the limit of dilute solution. Therefore, the excess chemical potentials μ_{conf} and μ_{bulk} were obtained for a single chain in a relatively large simulation box. The chemical potential was determined using a biased chain insertion method.[24]

The confined solution in most cases was represented by a slit pore, which is a cubic lattice with dimensions of $100 \times 100 \times (D + 1)$ along the x, y, and z directions. There are two solid walls separated by a distance of D in the z direction. No polymer beads may occupy the sites on the walls. Periodic boundary conditions are applied in the x and y directions. The bulk solution was represented by a cubic lattice with dimensions of $100 \times 100 \times 100$, with periodic boundary conditions applied in all three directions. Only the interactions of polymer beads with the pore walls were considered; hence polymer chains are considered to be in a good athermal solvent.

Several polymers were studied including homopolymer (A_N), AB diblock copolymers (A_NB_M), BAB triblock copolymers ($B_MA_NB_M$), and ABA triblock copolymers ($A_{N/2}B_MA_{N/2}$), where the subscripts denote the length of the blocks. Typically N and M range from 25 to 200. The radius of gyration R_g of a homopolymer A_N then ranges from 2.6 to 10.0 in the lattice unit. A slit pore with $D = 19$ would have a ratio $D/(2R_g)$ around 1−4 for the largest to the smallest chain being studied, a value typically encountered in experiments. In this study, "A" represents the visible block(s), which is (are) set in the size-exclusion mode, meaning the A monomer does not have any interactions with the wall ($\epsilon_{aw} = 0$) except for the hard core repulsion. "B" represents the invisible block(s), where the interaction of the B monomers with the surfaces ϵ_{bw} is set at the predetermined critical condition.

The location of the critical condition was investigated in two previous papers.[22,23] We defined the critical condition as the point at which the partition coefficient of a homopolymer (B) would have the least dependence on the chain length, in the same spirit as that done in experimental studies. We located the critical condition by plotting the deviations in the partition coefficients of a set of homopolymer chains with different lengths as a function of the surface/wall interaction. The minimum in the plot would correspond to the "critical condition" at which the partition coefficient of the homopolymers would have the least dependence on the chain length at that surface/wall interaction. For a slit pore,[22] the critical condition was found to be the same as the critical adsorption point, $\epsilon_w^{cr} = -0.276$, which was independently determined by studying the adsorption transition of an end-anchored polymer chain on a flat wall. For a square channel pore, the critical condi-

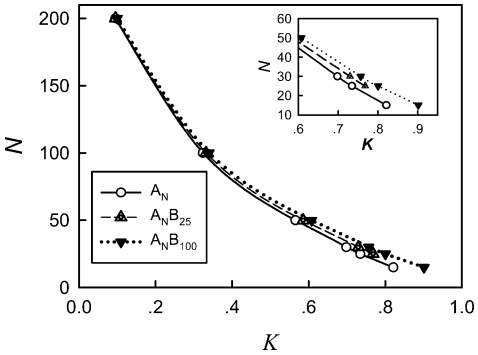

Figure 1. Plots of chain length N versus partition coefficient K in a slit pore of width $D = 19$ for homopolymer A_N, diblock copolymer A_NB_{25}, and diblock copolymer A_NB_{100}, where the A block is in exclusion mode ($\epsilon_{aw} = 0$) and the B block is at the critical condition ($\epsilon_{bw} = -0.276$). The inset shows the differences between the data sets at the lower part of the graph.

Table 1. Computational LCCC Characterizations of the A Block Length in a Diblock AB When the B Block Is Set at the Critical Condition in a Slit of Width $D = 19$

	LCCC measured length of A block (error[a])	
actual length of A block	length of B block = 25	length of B block = 100
25	21.2 (15%)	17.3 (31%)
30	26.0 (13%)	22.6 (25%)
50	46.3 (7%)	43.0 (14%)
100	96.0 (4%)	94.0 (6%)

[a] Error = $100[(N_{actual} - N_{calculated})/N_{actual}]$.

tion is shifted from the critical adsorption point and its exact location depends on the pore size.[23]

Results and Discussion

A. Comparison of Retention Behaviors for A_NB_M with A_N. Figure 1 compares the partition coefficients of a homopolymer A_N with that of a diblock copolymer A_NB_M, with $M = 25$ and 100 in a slit pore of width $D = 19$ with the B block set at the critical condition. For any given N, the partition coefficient of the diblock copolymer A_NB_M is greater than that of the homopolymer A_N. The difference between the two is larger when N is smaller and when the B block length is longer (the inset shows the difference between the data sets at the lower portion of the graph). If we assume that the quasi-equilibrium condition is held here, then the partition coefficient is directly proportional to the retention volume. A larger K implies a larger retention volume or a longer retention time. Then our data are in good agreement with the experimental results by Lee et al.[18] In their study, polystyrene/polyisoprene diblock copolymers (PS-*b*-PI) were employed in an LCCC analysis with a range of pore diameters from 100 to 1000 Å. They found that, by setting either the PS or PI blocks at the critical condition, the retention time of the PS-*b*-PI increased as the length of the invisible block increased at a constant length of visible block.

Table 1 displays errors in the estimated length of the visible block from a computational LCCC experiment. Here, the computationally determined dependence of K on N for a homopolymer was used as a calibration curve, and the visible block length of A in the AB diblock was estimated from the computationally determined K_{AB} value against the calibration curve. Thus the estimated A block length in an AB diblock copolymer differs from the actual length, by 4% at $N = 100$ to 15% at $N = 25$ when the B block length is 25, and 6% at $N = 100$ to 31% at $N = 25$ when the B block length is 100. Clearly, the longer the invisible block, the larger the error is. Also the shorter the visible block, the larger the percent error is. The same trend of dependence of percent errors in the estimated molecular weight of the visible block using LCCC was reported by Lee et al.[18] For example, at a constant length of the visible block PI (molecular weight ~12.5 kg/mol), the percent error increased from 4% to 16% when the molecular weight of the invisible block PS increased from 3.3 to 38.1 kg/mol. On the other hand, when the invisible block length was kept constant and the visible block length was varied, they found that the percent error in the estimated molecular weight of the visible block decreased from 33% to 2% when the molecular weight of the visible block increased from 3.0 to 34 kg/mol.

As stated earlier, previous theories based on the Gaussian chain model or the random walk chain would predict the retention behavior of a diblock A_NB_M to be the same as that of a homopolymer A_N and therefore LCCC characterization of the diblock copolymer should be accurate. The simulation reported here treats the chain as a self-avoiding walk chain that takes into account the excluded volume interaction. The inclusion of the excluded volume interaction in the simulation gives rise to the same phenomena seen in experiments. Hence we may conclude that these observed influences of the invisible block on the elution behaviors of the visible block are due to the excluded volume interaction ignored in previous theories.

A simple explanation of the observed effect can be given here. Let $\Delta\mu^{AB} = \mu^{AB}_{conf} - \mu^{AB}_{bulk}$ and $\Delta\mu^{A} = \mu^{A}_{conf} - \mu^{A}_{bulk}$ stand for the chemical potential differences of a diblock copolymer AB and a homopolymer A between the confined state and the bulk solution, respectively. The partition coefficients are given by $K_A = \exp(-\Delta\mu^A/RT)$ for the homopolymer and $K_{AB} = \exp(-\Delta\mu^{AB}/RT)$ for the diblock AB. To a first degree of approximation, one may assume that the confinement free energy of the diblock is the sum of the costs of confining each individual block:

$$\Delta\mu^{AB} \approx \Delta\mu^{A} + \Delta\mu^{B} \quad (1)$$

Then $K_{AB} = K_AK_B$. When the B block is set at the critical condition, if $\Delta\mu^B = 0$, then $K_B = 1$; therefore $K_{AB} = K_A$. Theories based on the Gaussian chain or the random walk chain would predict this. However, simulations of chains with the excluded volume interaction[22,23] have shown that, at the critical condition most likely employed in the LCCC experiment, $\Delta\mu^B \neq 0$, but $\Delta\mu^B < 0$, and hence $K_B > 1$. Therefore when the B block is set at the critical condition, $K_{AB} > K_A$, a result exactly observed here. Also from the earlier study, the longer the B block, the larger the K_B at the critical condition in a slit pore of $D = 19$ (note in a smaller pore, K_B could decrease with the chain length but remains greater than 1), hence the larger the difference between K_{AB} and K_A. On the other hand, when the visible block length increases, $\Delta\mu^A$ would increase. As a result, the effect of nonzero $\Delta\mu^B$ on the overall value of $\Delta\mu^{AB}$ would be relatively small since $\Delta\mu^{AB}$ will be dominated by the term $\Delta\mu^A$. Hence the influence of the invisible block on the elution behavior of a diblock with a longer visible block is relatively weak.

Table 2 illustrates how the slit width affects the characterization accuracy. With a decreased slit width,

Table 2. Computational LCCC Characterizations of the A Block Length in a Diblock AB at Different Slit Widths When the B Block Is Set at the Critical Condition

slit width D	actual length of A block	LCCC measured length of A block (error[a]) length of B block = 25	length of B block = 100
9	25	24.2 (3%)	23.2 (7%)
19	25	21.2 (15%)	17.3 (31%)
29	25	20.8 (17%)	17.3 (31%)
9	50	48.7 (4%)	47.8 (4%)
19	50	46.3 (7%)	43.0 (14%)
29	50	46.8 (6%)	43.8 (13%)

[a] Error = $100[(N_{\text{actual}} - N_{\text{calculated}})/N_{\text{actual}}]$.

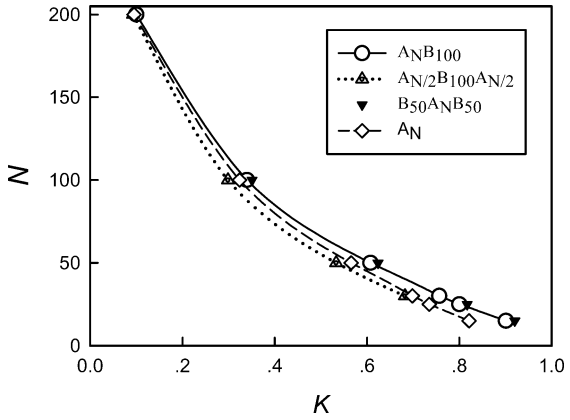

Figure 2. Plots of chain length N versus partition coefficient K in a slit pore of width $D = 19$ for homopolymer A_N, diblock copolymer A_NB_{100}, triblock copolymer $A_{N/2}B_{100}A_{N/2}$, and triblock copolymer $B_{50}A_NB_{50}$, at the same conditions as in Figure 1.

the visible block is more excluded from the pore; hence the elution behavior of the diblock is again dominated by the exclusion of the visible block from the slit, similar to the case when the length of the visible block increases at a constant slit width. This leads to a reduced error in the estimated length of the visible block in LCCC. Decreasing the slit width from $D = 19$ to $D = 9$ resulted in a decrease in the error of the estimated A block length from 17% to 3% for a chain with an actual A length of 25 and B invisible block length of 25. The errors seem to level off when the slit width increases from $D = 19$ to $D = 29$. Lee et al.[18] have used relatively larger pores compared with those of other experimental studies.[11] This could probably explain why Lee et al. observed these influences of the invisible blocks whereas others did not observe the same effect.

B. Retention Behaviors for Triblock Copolymers $A_{N/2}B_MA_{N/2}$ and $B_{M/2}A_NB_{M/2}$. Figure 2 compares the partition coefficients for a homopolymer of A_N, a diblock copolymer A_NB_{100}, a triblock $B_{50}A_NB_{50}$, and a triblock $A_{N/2}B_{100}A_{N/2}$ when N is varied from 15 to 200 in a slit pore of width $D = 19$. Note that these copolymers (excluding the homopolymer) are of the same total length and of the same chemical composition, just like the copolymers analyzed in Park et al.'s study.[19] The curve for the triblock copolymer of $A_{N/2}B_{100}A_{N/2}$ lies below that of the homopolymer A_N, while the curves for the diblock copolymer A_NB_{100} and the triblock $B_{50}A_NB_{50}$ lie almost on top of each other and they are above the curve for the homopolymer A_N. This indicates that ABA would elute earlier than the diblock AB and BAB, while AB and BAB would elute at almost the same time. This again is in perfect agreement with Park et al.'s observations. Table 3 shows our computational LCCC characterization of the length of A block in the triblocks ABA and BAB in a slit of width $D = 19$. The length of the A block is underestimated in BAB and is overestimated in ABA. The observed errors are comparable with the reported values of Park et al.[19] except for the cases when $N = 15$, where the error reached 75%.

Table 3. Computational LCCC Characterizations of the A Block in a Triblock ABA and BAB When the B Block Is Set at the Critical Condition in a Slit of Width $D = 19$

actual total length of A block	LCCC measured total length of A block (error[a]) $A_{N/2}B_{25}A_{N/2}$	$A_{N/2}B_{50}A_{N/2}$	$A_{N/2}B_{100}A_{N/2}$
30.0	33.7 (−12%)	33.2 (−11%)	32.3 (−8%)
50.0	55.3 (−11%)	55.3 (−11%)	54.8 (−10%)
100.0	104.6 (−5%)	104.4 (−4%)	104.6 (−5%)

actual length of the A block (N)	LCCC measured length of A block (error[a]) $B_{25}A_NB_{25}$	$B_{50}A_NB_{50}$	$B_{100}A_NB_{100}$
15.0	6.9 (54%)	3.8 (75%)	3.7 (75%)
25.0	17.5 (30%)	15.3 (39%)	16.9 (32%)
50.0	42.3 (15%)	40.5 (19%)	45.2 (10%)
100.0	92.2 (8%)	91.2 (9%)	96.2 (4%)

[a] Error = $100[(N_{\text{actual}} - N_{\text{calculated}})/N_{\text{actual}}]$.

The differences in the partition coefficients disappeared when the visible block length increased to $N = 200$, as is evident in Figure 2. With a long visible block, the copolymer is in the strong exclusion mode and the partition coefficient will be dominated by the exclusion of the visible block from the pore. The invisible blocks would exert little effect. The differences in the partition coefficients of these copolymers are pronounced only when the visible block is relatively small compared to the pore size.

These results suggest that the observed effect of invisible blocks on the elution behavior of ABA and BAB at the critical condition in Park et al.'s study could be attributed to the thermodynamic origin. If we apply the same approximation to BAB as in the previous section, namely, $\Delta\mu^{BAB} = \Delta\mu^B + \Delta\mu^A + \Delta\mu^B$ (i.e., the confinement free energy of the copolymers is the sum of each individual block), then we would have $K_{BAB} = K_BK_AK_B$. Knowing that when B is at the critical condition, $K_B > 1$, then we would have $K_{BAB} \approx K_{AB} > K_A$, agreeing with what was observed here. However, when applied to ABA, it would lead to the prediction, $K_{ABA} = K_{BAB} > K_A$, completely inconsistent with the simulation results. Apparently a different mechanism is in operation for ABA triblock copolymers. The theoretical calculations by Guttman et al.[16] with the random walk chain model have also shown that $K_{ABA} < K_A$. They have concluded that the partition rule for ABA copolymer when B is invisible does not reduce simply to that of homopolymer and no general rules could be proposed for ABA, unlike the results for BAB and AB copolymers. Recently Gorbunov and Vakhrushev[17] examined the partitioning of multiblock copolymers and star-shaped copolymers $(AB)_n$ with the Gaussian chain model. They have also found that, when the visible blocks are separated by the invisible blocks, the partition coefficient of the multiblock copolymers depends on the invisible block. Our simulation results for ABA therefore reflect the same topological effect observed in these theoretical calculations. It seems that $\Delta\mu_{conf}$ for the block copolymers can be expressed as a sum of the contributions from individual blocks when the invisible block is divided into different segments, but not when the visible block is divided into different segments.

Some insights can be gained from the density profiles of these polymers in the slit. Figure 3a shows the

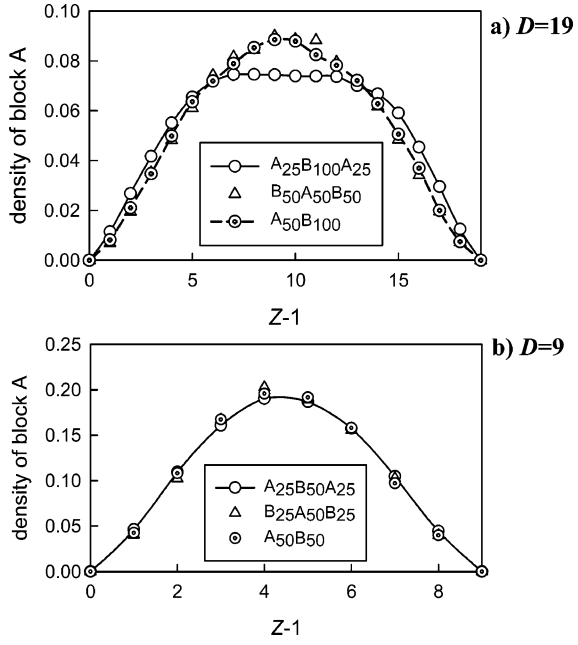

Figure 3. Density distributions of A block in three block copolymers AB, ABA, and BAB along the direction perpendicular to the walls in a slit pore of width (a) $D = 19$ and (b) $D = 9$.

density distribution of the A block(s) in the three types of copolymers, $A_{25}B_{100}A_{25}$, $B_{50}A_{50}B_{50}$, and $A_{50}B_{100}$, along the direction normal to the walls in a slit pore of width $D = 19$. In general, a nonadsorptive chain when confined between two walls tends to avoid the walls, leading to an accumulation of density distributions in the middle of the slit, as shown in Figure 3a. Interestingly, no significant differences are observed between the density distributions of the A blocks in AB and BAB copolymers, but the density distribution of the A blocks in ABA is much flatter than the other two and has fewer accumulations in the middle of the slit. The A blocks in ABA copolymer are found near the wall more than the other two types, as if the A blocks in ABA are unable to avoid the walls. The invisible B block, being in the middle of ABA, effectively pushes the two A blocks toward the walls. We may therefore envision that the visible A blocks in ABA copolymers feel a stronger confinement imposed by the walls and hence have a higher free energy of confinement which results in a smaller K_{ABA}. This explanation is further supported by data in a smaller pore. Figure 3b shows the density distributions of the visible A blocks of the three types of block copolymers in a slit of width $D = 9$. Now there is no difference in the density distributions. Interestingly, the partition coefficients of these copolymers in $D = 9$ did not show any difference, either, as presented in Figure 4. Therefore, the difference in partition coefficient is linked directly to the difference in density distributions of the visible blocks in the slit. When the density distributions of the visible blocks in the slit are the same, then the partition coefficients are likely the same. We give an illustrative drawing in Figure 5 to show how the visible blocks in ABA copolymers may distribute in a wide slit versus in a narrow slit. In a narrow slit, each invisible block is confined by the slit (i.e., the confinement blob is smaller than the visible block). Hence the density profile of the visible block in ABA will exhibit a pattern similar to that of the visible block alone. In a wide slit, the confinement scale is larger than the individual blocks and as a result the

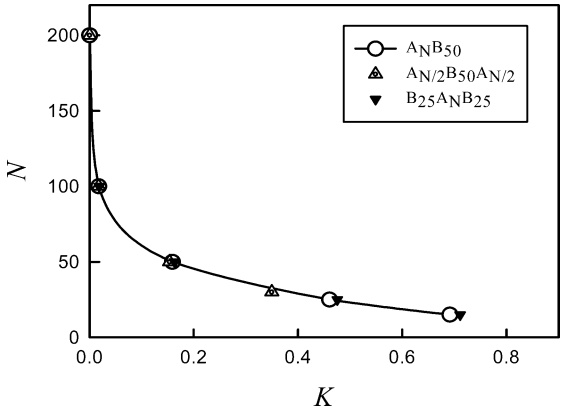

Figure 4. Plots of chain length N versus partition coefficient K in a slit pore of width $D = 9$ for diblock copolymer A_NB_{50}, triblock copolymer $A_{N/2}B_{50}A_{N/2}$, and triblock copolymer $B_{25}A_NB_{25}$.

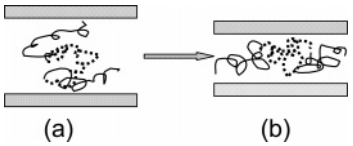

Figure 5. Schematic illustration of triblock copolymer chain ABA confined in (a) a wide pore and (b) a narrow pore. The solid line represents the A block chain, and the dotted line represents the B block chain.

density profile is determined by both the visible and invisible blocks. Thus the invisible block could have an influence on the partition coefficients of the copolymers.

For the diblock AB copolymer, we have observed that an increase in the invisible block length generally leads to a larger difference between K_{AB} and K_A. However, for the triblocks ABA and BAB, we could not observe a general rule when the length of the invisible block increased. Data in Table 3 show almost no or little effect on the observed errors when the invisible block length was increased. We believe part of the reason is due to the lack of adequate accuracy in the determined K values for these triblocks. When the total chain length increases, the errors associated with the determined values for μ_{conf} and μ_{bulk} also increase and this leads to a larger uncertainty in the determined K value. This inhibits us from an accurate assessment of the effect of increase in the invisible block length on the elution behavior of the triblocks.

C. Simulation Results in a Square Channel. The above reported simulation results were obtained in a slit pore. We have shown earlier that the critical condition in a slit pore is the same as the critical adsorption point, but in a square channel, it shifts with the channel width.[23] Hence it is of interest to examine if the above observed elution behavior of copolymers would depend on the pore geometry. For that purpose we have examined the partition of these copolymers in a square channel of width $D = 19$. The critical condition in a square channel of $D = 19$ was at $\epsilon_w^{cc} = -0.284$ as determined earlier.[23] When the B block was set at this critical condition, $\epsilon_{bw} = -0.284$, we found the same elution pattern; the line for ABA lies below that of A homopolymer, and that for BAB lies above that of A homopolymer (data not shown). The pattern does not change when the invisible block length changes. However, if we set $\epsilon_{bw} = -0.276$ instead (off the critical condition), the elution pattern changes when the length of the invisible block changes. When the invisible block

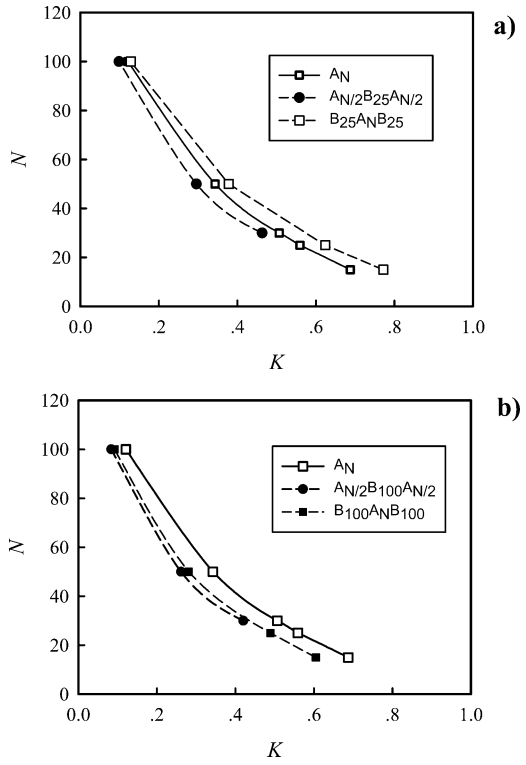

Figure 6. Plots of chain length N versus partition coefficient K in a square channel pore of width $D = 19$. The A block is in the exclusion mode ($\epsilon_{aw} = 0$), and the B block ($\epsilon_{bw} = -0.276$) is off the critical condition point (see the text for discussion). (a) Homopolymer A_N, triblock copolymer $A_{N/2}B_{25}A_{N/2}$, and triblock copolymer $B_{25}A_NB_{25}$; (b) homopolymer A_N, triblock copolymer $A_{N/2}B_{100}A_{N/2}$, and triblock copolymer $B_{100}A_NB_{100}$.

B is short (i.e., B block length is 25), then the line for BAB lies above that of the homopolymer A, and the line of ABA lies below that of A, the same pattern as before (data are shown in Figure 6a). When B is longer (i.e., B block length is 100), the line of BAB lies below that of A homopolymer and the line of ABA lies further below that of the homopolymer, as shown in Figure 6b. This behavior can be understood when one realizes that, at $\epsilon_{bw} = -0.276$, the B block is not in the critical condition in a square channel of width $D = 19$. The B block could be in the exclusion mode when its length is long. Hence, with a longer B block, the line for BAB could lie below that of A because B is also in the exclusion mode and ABA would lie even further below. These results further confirm that our definition of the critical condition is more appropriate. Simply equating the critical adsorption point as the critical condition is not appropriate. The elution patterns of these copolymers observed in the simulations would remain the same as long as one finds the right critical condition. However, with a slightly shifted condition, one may observe an altered pattern.

Conclusions

This study examined the effect of invisible blocks on the elution behavior of copolymers in LCCC through computer simulations of self-avoiding walk chains. The simulation results are in excellent agreement with reported experimental results. The invisible block(s) of copolymers affect the elution of the visible blocks. The extent of this affect is unique for each architectural type. For a diblock copolymer AB, the presence of the invisible B block would increase the elution time of the visible block A. Similarly, the presence of the invisible B blocks increases the elution time of BAB triblock. However, for an ABA triblock, the presence of the invisible B block lowers the elution time of the visible blocks if the visible blocks are treated as connected without the presence of the B block. These observed influences could be attributed to two different origins. For AB and BAB types where the visible block A remains as a single block, we can attribute the difference of K_{AB} and K_{BAB} from K_A to the origin that $K_B > 1$ when the B block is at the critical condition for a self-avoiding walk chain. However, for a random walk chain, $K_B = 1$ when B is at the critical condition; hence theories based on the random walk chain fail to predict any difference between K_{AB} and K_{BAB} from K_A. When the visible block is separated into two blocks such as in ABA, then both the self-avoiding walk chain model (used in the simulation) and the random walk chain model (used in the theory) predict $K_{ABA} < K_A$. The origin of the latter relationship is in the chain connectivity which both simulations and theories have accounted for. These observed effects, however, tend to disappear when the visible block length is longer or the size of the pore is smaller; then the elution will be dominated by the exclusion of the visible block from the pore and the invisible blocks would exert little influence.

The agreement between the simulation results and experiments is also remarkable. Not only are the qualitative trends in complete agreement, but also the quantitative values are comparable. As a result, several things can be said. First, the elution of polymers in these chromatographic studies is largely controlled by the equilibrium partitioning; transport seems to have little effect on the separations. Second, theory based on the Gaussian chain model captures most features of the elution pattern in these interactive chromatographic separations, although inclusion of the excluded volume interaction in the chain can bring the predictions from the simulation (or the theory) to a better agreement with the experimental results. This study also confirms that effects observed in experiments by Chang's group are genuine and can be traced to be of thermodynamic origin.[18,19] They are likely to be observed in the wide pore with relatively small visible blocks, and the effect may disappear in small pores with large visible blocks. Hence, experimental studies with different conditions may result in different conclusions about the accuracy of the LCCC.

References and Notes

(1) Bates, F.; Fredrickson, G. *Annu. Rev. Phys. Chem.* **1990**, *41*, 525−527.
(2) *Introduction to Block Copolymers*; Hamley, I. W., Ed.; Wiley: New York, 2004.
(3) *Polymers for Controlled Drug Delivery*; Schmolka, I. R., Ed.; CRC Press: Boston, 1991.
(4) Zipfel, J.; Lindner, P.; Tsianou, M.; Alexandridis, P.; Richtering, W. *Langmuir* **1999**, *15*, 2599−2602.
(5) Thurn-Albrecht, T.; Schotter, J.; Kastle, G. A.; Emley, N.; Shibauchi, T.; Krusin-Elbaum L.; Guarini, K.; Black, C. T.; Tuominen, M. T.; Russell, T. P. *Science* **2000**, *290*, 2126−2129.
(6) Retsos, H.; Margiolaki, I.; Messaritaki, A.; Anastasiadis, S. H. *Macromolecules* **2001**, *34*, 5295−5305.
(7) Retsos, H.; Anastasiadis, S. H.; Pispas, S.; Mays, J. W.; Hadjichristidis, N. *Macromolecules* **2004**, *37*, 524−537.
(8) Svensson, B.; Olsson, U.; Alexandridis, P. *Langmuir* **2000**, *16*, 6839−6846.
(9) Pasch, H.; Trathnigg, B. *HPLC of Polymers*; Springer-Verlag: Berlin, 1999.

(10) Zimina, T. M.; Kever, J. J.; Melenevskaya E. Y.; Fell, A. F. *J. Chromatogr.* **1992**, *593*, 233−241.
(11) Falkenhagen, J.; Much, H.; Stauf, W.; Muller, A. H. E. *Macromolecules* **2000**, *33*, 3687−3693.
(12) Janco, M.; Hirano, T.; Kitayama, T.; Hatada, K.; Berek, D. *Macromolecules* **2000**, *33*, 1710−1715.
(13) Lee, H. C.; Lee, H.; Lee, W.; Chang, T. H.; Roovers, J. *Macromolecules* **2000**, *33*, 8119−8121.
(14) Gorbunov, A. A.; Skvortsov, A. M. *Vysokomol. Soedin. Ser. A* **1988**, *30*, 453−458.
(15) Gorbunov, A. A.; Skvortsov, A. M. *Vysokomol. Soedin. Ser. A* **1988**, *30*, 895−899.
(16) Guttman, C. M.; Di Marzio, E. A.; Douglas, J. F. *Macromolecules* **1996**, *29*, 5723−5733.
(17) Gorbunov, A. A.; Vakhrushev, A. V. *J. Chromatogr., A* **2005**, *1064*, 169−181.
(18) Lee, W.; Cho, D. Y.; Chang, T. Y.; Hanley, K. J.; Lodge, T. P. *Macromolecules* **2001**, *34*, 2353−2358.
(19) Park, I.; Park, S.; Cho, D.; Chang, T.; Kim, E.; Lee, K.; Kim, Y. J. *Macromolecules* **2003**, *36*, 8539−8543.
(20) Chen, Z.; Escobedo, F. *Phys. Rev. E* **2004**, *69*, 218021−2180210.
(21) Cifra, P.; Bleha, T. *Polymer* **2000**, *41*, 1003−1009.
(22) Gong, Y.; Wang, Y. *Macromolecules* **2002**, *35*, 7492−7498.
(23) Orelli, S.; Jiang, W.; Wang, Y. *Macromolecules* **2004**, *37*, 10073−10078.
(24) Mooij, G. C. A. M.; Frenkel, D. *Mol. Phys.* **1991**, *74*, 41−47.

MA050899A